ACS OMEGA

http://pubs.acs.org/journal/acsodf

Article

Effects of Associated Minerals on the Co-Current Oxidizing Pyrolysis of Oil Shale in a Low-Temperature Stage

Qinchuan Yang, Mingyi Guo, and Wei Guo*

Cite This: *ACS Omega* 2021, 6, 23988−23997

Read Online

ACCESS | Metrics & More | Article Recommendations

ABSTRACT: Low-temperature co-current oxidizing pyrolysis, which can achieve high recovery of hydrocarbons without significant oil loss, has great potential to reduce the huge external energy required for oil shale conversion. However, this promising method is far from being fully understood, especially the unknown competing mechanism of different types of inorganic minerals in promoting or inhibiting hydrocarbon generation. In this study, the raw Huadian oil shale (HD-R), its carbonate-free (HD-C-F), and carbonate-silicate-free (HD-CS-F) samples obtained through acid treatment are used to investigate the effects of associated minerals on the oil shale co-current oxidizing pyrolysis. The results of shale oil yields of HD-R, HD-C-F, and HD-CS-F were 41.53, 22.38, and 33.97%, respectively, indicating that silicates inhibited, while carbonates catalyzed the formation of shale oil during the co-current oxidizing pyrolysis. Meanwhile, silicates increase the alkane content and decrease the alkene content in shale oil via promoting the combination of hydrogen radicals and alkyl radicals. On the contrary, alkali metals and alkaline earth metals in carbonates inhibit the binding activity of hydrogen radicals and alkyl radicals, concurrently enhancing the release of hydrogen-free radicals of alkyl radicals to form more alkenes. The removal of carbonates could enhance the conversion of organic carbon into hydrocarbons, and the silicates will strengthen the conversion process. It is hoped that this experiment can further enrich and perfect the basic theory of oil shale pyrolysis and provide a reliable reference for the pretreatment of oil shale conversion.

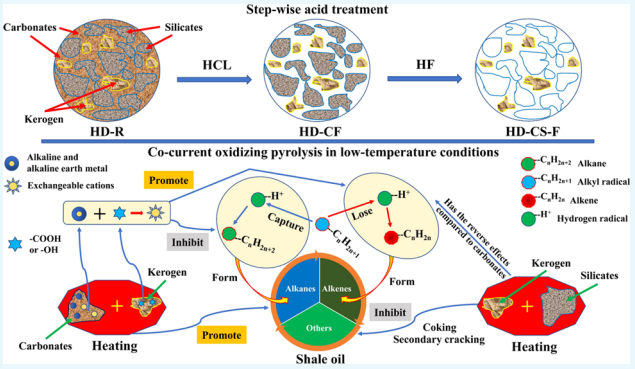

1. INTRODUCTION

Oil shale, a kind of unconventional petroleum resource with massive reserves, has attracted more attention in the last few years due to the contradiction between the increasing global energy consumption and shortage of conventional non-renewable fossil fuels, such as crude oil, coal, and natural gas,[1] which is 10 times more than the liquid petroleum reserves, making it a great potential to become an alternative for conventional fossil energy.[2]

The kerogen, contained with a proportionally large amount in oil shale, can be converted into hydrocarbons by thermal degradation, which is the prevalent method of oil shale utilization.[3,4] However, the thermal decomposition of oil shale requires high energy input, such as heating crude oil shale to 550 °C with 700 °C hot carrier gas, which is the most challenging obstacle to oil shale pyrolysis.[5] Therefore, to achieve the highly effective transforming utilization of oil shale, much efforts have been devoted to the characteristics of oil shale pyrolysis. Our group demonstrated a low-energy topochemical reaction strategy,[6,7] which is different from physical heating or complete combustion. In the process of topochemical reaction, sufficient heat could be released from the partially oxidized kerogen and thus accelerate the self-cracking of kerogen. Guo et al. developed a retorting route with low-energy input using low-temperature hot carrier gas, which was also realized through a self-heating effect; that is, the retorting temperature was automatically increased without external heat supply.[8,9]

Fortunately, based on the topochemical reaction strategy, we developed the co-current oxidizing pyrolysis using pure oxygen to enhance the oxidation heat release of semicoke without remarkable oil loss at low conversion temperatures.[10] The results showed that about 82% oil (oil yield is 15%) could be obtained at 350 °C compared to the Fischer assay result (18.31%). Although this novel method is particularly promising and has great potential to reduce the huge external energy input, detailed information has not been studied yet;

Received: June 12, 2021
Published: September 7, 2021

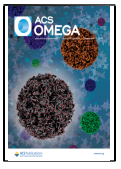

Table 1. Results of Proximate and Ultimate Analyses of the Raw Oil Shale and Its Demineralized Samples

	proximate analysis (wt %, ad)				ultimate analysis (wt %, dmmf)				
sample	M	A	V	FC[a]	C^{o}[b]	C^{i}[c]	H	S	N
HD-R	4.22	52.36	41.84	1.58	32.78	3.85	3.68	1.75	0.56
HD-C-F	1.26	37.43	51.43	9.88	38.56	0.11	3.56	1.38	0.62
HD-CS-F	1.08	7.85	70.09	20.98	47.67	0.07	3.58	1.94	0.84

[a]Calculated by difference. [b]C^{o}: organic carbon. [c]C^{i}: inorganic carbon.

many crucial factors that may affect the pyrolysis behavior and product distribution need to be investigated.[5]

As is well known, the decomposition of kerogen and minerals coincides due to the high mineral content and the compact distribution of kerogen and minerals, which will cause a significant interference to the thermal cracking of oil shale.[11−14] Several studies have focused on the thermal behavior and product composition during the co-pyrolysis of oil shale and its associated minerals. For example, Borrego et al. conducted a thermogravimetric analysis of oil shale in different mining areas in Spain[15] and concluded that the mineral matrix offers a catalytic effect on the release of kerogen pyrolysis products. Balice reported that the catalytic effect of carbonate on kerogen decomposition was not apparent while the inhibition of silicate was significant,[12] and the previous studies revealed that the elimination of carbonates decreased the hydrocarbon yield while the removal of silicate minerals had the opposite effect.[16] However, more workers have found that the activation energy of oil shale pyrolysis was significantly higher compared to kerogen; that is, minerals inhibited the pyrolysis of organic matter.[17−19] Wang et al. pointed out that carbonate could promote the conversion of organic carbon and hydrogen into shale oil, while silicate had an inhibitory effect on the process, and the inhibition is more potent.[20,21] Meanwhile, some researchers determined that kerogen−mineral interactions are primarily nonbonded via extensive investigations on kerogen−mineral interactions in the Green River oil shale.[22−24] Several experiments also demonstrated from the results of Fourier transform infrared spectroscopy and Liquid chromatography fractionation of oil shale that carbonate minerals primarily interact with carboxylic acids, while silicate minerals form Si−O ether bonds.[25] The above-mentioned different results reveal that the thermal decomposition of organic matter in oil shale is extremely complicated, especially on the effect of the unknown competing mechanism of different types of inorganic minerals in promoting or inhibiting hydrocarbon generation.

Therefore, in the process of possible research and application of the new and efficient method of co-current oxidizing pyrolysis, it is particularly critical to determine the influence of associated minerals on the thermochemical conversion behavior of organic matter to achieve the goal of "low-energy input and high-efficiency recovery", especially the application of this method in the in situ transformation of oil shale in reservoir scale. In this work, the potential effects of associated minerals on the co-current oxidizing pyrolysis of Huadian oil shale have been investigated at a low-temperature stage. First, hydrochloric acid and hydrofluoric acid were selected to eliminate the carbonates and silicates in oil shale, and the corresponding demineralized products were obtained. Then, the pyrolysis experiment of the original oil shale and its demineralized products in co-current oxidizing conditions was carried out. Meanwhile, detailed information about the physicochemical properties of the experimental objects and pyrolytic products were obtained by a variety of advanced testing instruments. In this way, the effects of inorganic minerals on the structure, pyrolysis behavior, and distribution characteristics of pyrolytic products of oil shale during the low-temperature co-current oxidizing pyrolysis were studied.

2. RESULTS AND DISCUSSION

2.1. Characterization of Raw Oil Shale and the Demineralized Products. The results of ultimate and proximate analyses of the raw samples and their demineralized products are summarized in Table 1. It shows that the ash was 52.36% for HD-R and decreased to 37.43 and 7.85% after successive acid washing treatment. The fixed carbon and volatile matter were increased significantly from 1.58 to 20.98% and 42.84 to 70.09%, respectively, when most of the minerals were removed. Meanwhile, the organic carbon in samples was increased from 32.78% (HD-R) to 47.67% (HD-CS-F) with the elimination of carbonates and silicates by HCl/HF treatment, while the decrease of inorganic carbon that concentrated in minerals was due to the removal of large amounts of carbonates.[21] The X-ray diffraction (XRD) patterns containing necessary information of oil shale samples are displayed in Figure 1. As can be seen from the figure that

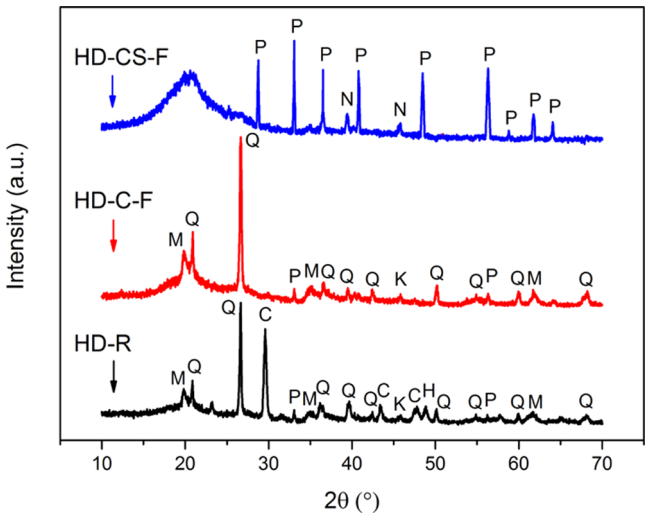

Figure 1. XRD patterns of HD-R, HD-C-F, and HD-CS-F samples. (Q: quartz; C: calcite; P: pyrite; M: montmorillonite; K: kaolinite; N: $NaMgAlF_6H_2O$; H: hematite).

the main minerals in HD-R include quartz (SiO_2), calcite ($CaCO_3$), montmorillonite, and pyrite (FeS_2), followed by a small amount of hematite (Fe_2O_3) and kaolinite. In general, the X-ray diffraction intensity of various substances in oil shale is not only associated with the relative content of the substance but also the crystallinity. In addition, the crystallinity is also positively correlated with the sharpness of the peak.[26] Therefore, it is clear that the quartz and calcite have higher

https://doi.org/10.1021/acsomega.1c03098
ACS Omega 2021, 6, 23988−23997

crystallinity in the obtained oil shale, while the low diffraction of kaolinite, montmorillonite, and other minerals was observed. The diffraction peaks of calcite at 29.5, 43.3, and 47.8° were disappeared in the HD-C-F sample, indicating that carbonate minerals were removed by hydrochloric acid. The quartz, montmorillonite, and kaolinite were eliminated by hydrofluoric acid, as confirmed.[27] Meanwhile, a broad characteristic absorption band that appeared between 15 and 25° can be attributed to the aliphatic carbon that existed in organic matter, and several low peaks that were observed at 39 and 44° can be associated with a fluoride compound ($NaMgAlF_6H_2O$).[28]

It is well known that chemical reactions, such as gasification, pyrolysis, and combustion of fossil fuels, mostly occurred in the interior and pores of rock.[29] Therefore, the evolution of the pore structure that occurred in oil shale with acid treatment is essential for the calculation of the heat transfer process, the reactive activity of organic matter, the migration of volatile substances, and the percolation process of fluid products.[30,31] Nitrogen adsorption/desorption is a widely used method that focuses on the investigation of pore structure, shape, and connectivity of conventional fossil energy, particularly for mesopores (2−50 nm) and micropores (<2 nm) that mainly existed in oil shale.[31] The curves shown in Figure 2a are typical anti-S type II isotherms according to the classification by Brunauer−Deming−Deming−Teller[32] and IUPAC, indicating that oil shale and demineralized products have more continuous complicated pores. When the relative pressure is less than 0.6, the adsorption branches of isotherm and desorption branches of isotherm basically coincide. Then, a hysteresis ring that can provide a large amount of pore structure information is generated as the relative pressure increases. Moreover, the hysteresis loops have decreased with the removal of minerals from oil shale, indicating that the removal of minerals has a vital effect on the pore structure of oil shale and made the adsorption capacity of samples reduce. It is noted that a slow growth appears in the adsorption branches of all of the isotherms as the pressure is lower than 0.9. Along with the increase of the relative pressure (P/P_0 > 0.9), the adsorption capacity increases obviously, which is caused by the capillary condensation of nitrogen when the relative pressure does not exceed the saturation pressure.

The characteristics of micropores and mesopores of the samples are also investigated by the nitrogen adsorption/desorption method. The distribution of pore size and specific surface area of oil shale and the demineralized products are given in Figure 2b,c, respectively. It can be seen that the minerals have a very important influence on the distribution of pore size of oil shale. The relative number of micropores and mesopores of HD-C-F obviously decreases while slightly increases after the removal of silicates, compared with the HD-R sample. The variation of the specific surface area distribution of the sample is similar to that of the pore diameter distribution. Table 2 shows the pore structure characteristic parameters of oil shale and the demineralized products. It shows that the removal of minerals first reduced the Brunauer−Emmett−Teller (BET) surface area of the sample from 4.886 to 2.301 cm^2/g and then increased to 5.461 cm^2/g. Meanwhile, there are the same variation characteristics of the single point surface area and point volume of the sample.

2.2. Distribution Characteristics of Pyrolytic Products. Figure 3 shows the special effect of demineralization on product distribution of oil shale pyrolysis in low-temperature co-current oxidizing conditions. It can be seen from Figure 3a

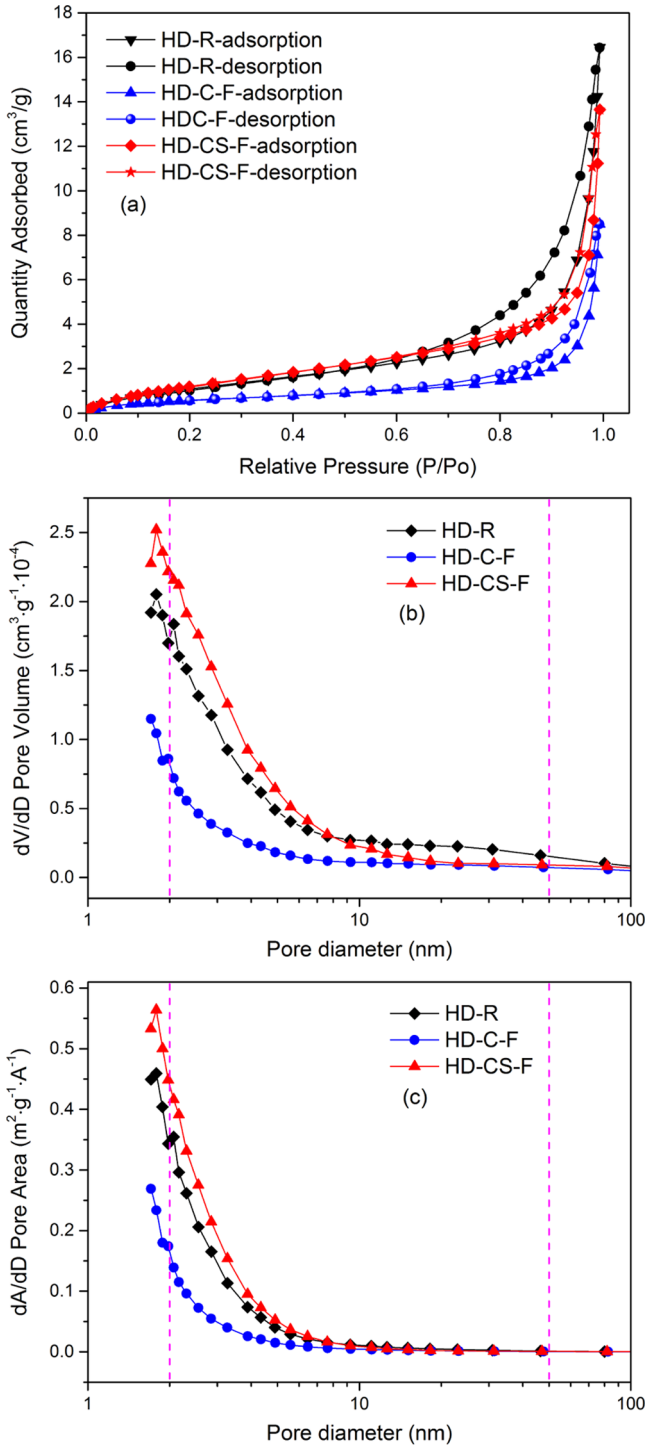

Figure 2. Pore structure characteristic curves of the raw oil shale and its demineralized products. (a) N_2 adsorption/desorption isotherms, (b) pore size distribution, and (c) specific surface area distribution.

Table 2. Pore Structure Parameters of Raw and Demineralized Oil Shale Samples

sample	BET surface area (cm^2/g)	single point surface area (cm^2/g) (at P/P_0 = 0.301)	pore volume (cm^3/g) (at P/P_0 = 0.993)
HD-R	4.886	4.174	0.025
HD-C-F	2.301	2.091	0.013
HD-CS-F	5.461	4.650	0.021

https://doi.org/10.1021/acsomega.1c03098
ACS Omega 2021, 6, 23988−23997

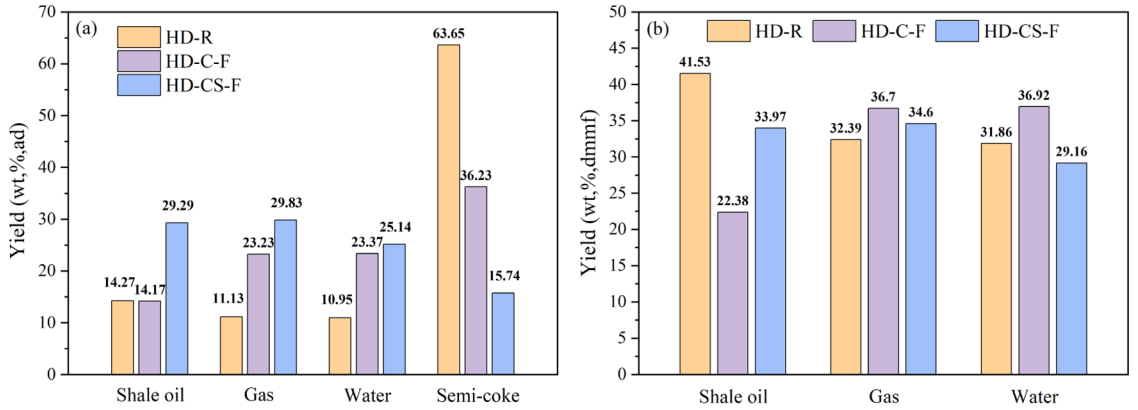

Figure 3. Yields of pyrolytic products of HD-R, HD-C-F, and HD-CS-F samples. (a) Dry basis, (b) dry weight, and mineral matter-free basis.

that the elimination of minerals has evidently affected the distribution of pyrolytic products of oil shale. The elimination of carbonate minerals resulted in a significant increase in gas and water yield but a marked decrease in semicoke yield. Moreover, it is noted that the rise in oil yield for HD-CS-F is measurable, which may be due to the organic components that became more concentrated with the removal of the most mineral matrix.[33] Changes in the composition of the oil shale will result in differences in the basis selected for the calculation of the pyrolytic products. Therefore, as shown in Figure 3b, the yields of pyrolytic products such as shale oil, water, and gas were uniformly calculated on a dry and mineral matter-free basis (dmmf). The results show that there was an apparent decrease in the oil yield for HD-C-F compared with the raw oil shale, and further elimination of silicates made the yield of shale oil increase from 23.28 to 29.87%, suggesting that carbonates had catalysis on the formation of shale oil during the co-current oxidizing pyrolysis, while the presence of silicate minerals inhibited the thermal decomposition of organic matter. However, unfortunately, clay minerals in silicates will cause a decrease in the recovery of volatile and total hydrocarbons via the secondary cracking and coking of products.

Meanwhile, Figure 3b also clearly indicates that the removal of carbonates resulted in an increase in gas and water yield for HD-C-F, while there was a decrease in their yield after the silicates were removed. Part of the reason is that the minerals present in the raw oil shale can make a contribution to the formation of gas and water. For example, some carbonate minerals can be decomposed into carbon dioxide, and the interlayer water and structural water in clay minerals will evaporate during pyrolysis.[4] However, the more critical reason is that the oxidation heat of semicoke is mainly utilized to provide energy for the decomposition of organic matter in co-current oxidizing pyrolysis of oil shale,[10] which means that it is difficult to avoid large amounts of organic matter being oxidized in an oxidizing atmosphere as the occurrence environment has changed significantly after acid washing. Therefore, unlike conventional retorting, the gas and water products are not only derived from the thermal decomposition of the organic matter and minerals but also closely related to the degree of oxidation of the organic matter in an oxidizing atmosphere. Furthermore, the results of nitrogen adsorption/desorption (as indicated above) showed that both the quantity and particle size of pores have increased slightly for HD-CS-F and appreciably reduced for HD-C-F after the elimination of considerable minerals, which resulted in a decrease in the particle size of oil shale and a narrower gap between particles. This greatly prolonged the retention time of pyrolytic products between the oil shale particles and hindered their release. Consequently, it allows more volatile hydrocarbons to be oxidized and enhances the second reaction of products. Therefore, the combined effects of temperature, catalysis, and inhibition of minerals, as well as the oxidation of organic matter and other potential factors, resulted in the diverse distribution characteristics of pyrolytic products for raw and demineralized oil shales.

The element distribution of the raw oil shale and its demineralized products before and after oxidative pyrolysis are displayed in Table 3. The organic functional groups in oil shale

Table 3. Element Distribution of Raw Oil Shale and Its Demineralized Products Before and After Oxidative Pyrolysis[a]

sample	C°	H	S	N
HD-R	32.78	3.68	1.75	0.56
HD-R-*OP	6.89	0.70	1.69	0.31
HD-C-F	38.56	3.56	1.38	0.62
HD-C-F-*OP	7.71	0.68	1.29	0.41
HD-CS-F	47.67	3.58	1.94	0.84
HD-CS-F-*OP	8.59	0.72	1.91	0.53

[a]C°: organic carbon. *OP: the sample after oxidative pyrolysis.

continue to fracture and recombine as the temperature increases during the thermal decomposition, resulting in significant changes in the chemical composition of the samples before and after thermochemical conversion. It can be seen from the results in the table that the carbon and hydrogen elements in the sample have been significantly reduced after oxidative pyrolysis. This is not only related to the thermal hydrocarbon expulsion of a large number of organic substances but also contributes to the oxidative exothermic reaction of the residual carbon in the semicoke during the process of oxidative pyrolysis, which is consistent with our previous study.[10]

2.3. Characterization of Shale Oils and Noncondensable Gases. Shale oil is a kind of brown viscous liquid product with a particular pungent smell generated through the thermal decomposition of organic matter. Similar to crude oil, shale oil is rich in alkanes and aromatics,[34] but contains more alkenes and has nonhydrocarbon components containing oxygen, nitrogen, sulfur, etc. Our previous study pointed out

https://doi.org/10.1021/acsomega.1c03098
ACS Omega 2021, 6, 23988−23997

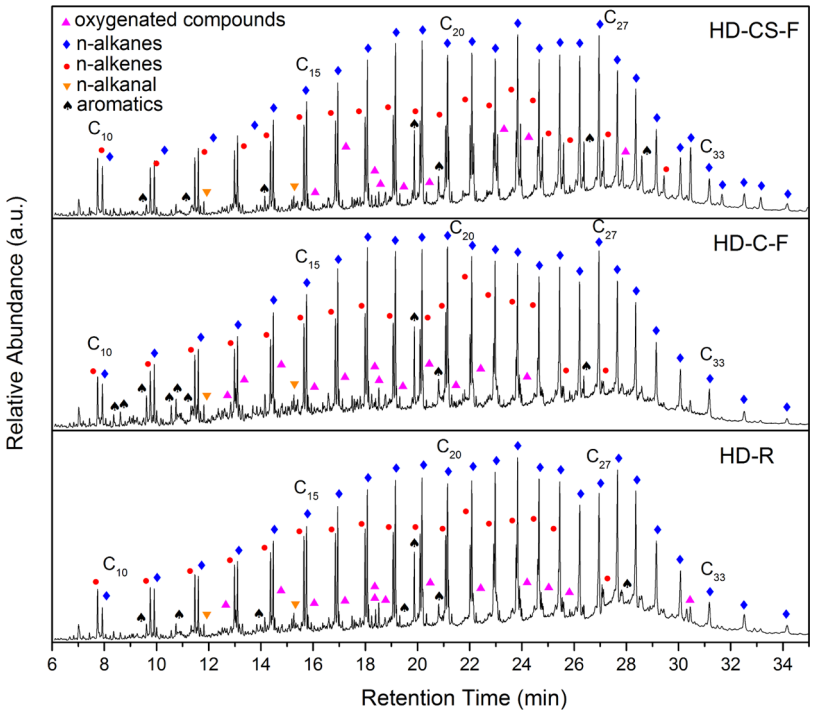

Figure 4. Total ion chromatogram (TIC) from GC−MS of the shale oils obtained during the thermal decomposition of oil shale.

that the shale oil generated in the co-current oxidizing pyrolysis conditions has more lighter components,[10] this may be related to the high temperature generated by the exothermic oxidation of semicoke, promoting the fracture of the C−C chemical bond to create more light components.[5] Therefore, it is of great significance to analyze the chemical composition characteristics of liquid hydrocarbons (shale oils) and noncondensable gases obtained from the raw and demineralized oil shales during the co-current oxidizing pyrolysis.

2.3.1. Analysis of Shale Oils. The features of shale oils obtained were first investigated with the gas chromatography−mass spectrometry (GC−MS) technique. The corresponding chromatograms of the shale oils derived from raw samples and their demineralized products are compared in Figure 4. The results showed that a great deal of hydrocarbons and derivatives were found in all of the obtained oils, such as aliphatic hydrocarbons (alkanes, alkenes, alkanal), aromatic hydrocarbons, and oxygenated compounds (alcohols, acids, ketones, etc.). Meanwhile, the n-alkanes with homologous series peaks dominated in all chromatograms, and each peak of n-alkanes was usually accompanied by the corresponding linear alkene peak.[6,33]

The relative content of the identified compounds in shale oils can be calculated by the ion current peak area, and the results, which have been normalized to 100%, are presented in Figure 5. What needs to be specially pointed out is only the substances with a peak area of more than 1% that were counted. It can be seen that the aliphatic alkanes belonging to saturated aliphatic hydrocarbons are dominant in all of the oils obtained, which is well consistent with the previous reports.[5,6,33] The content of alkanes increased from 62.59 to 64.65% with the removal of carbonates, while that for alkenes decreased from 24.79 to 18.83%, suggesting that the presence of carbonates resulted in a decrease in alkanes and an increase in alkenes. With most of the silicates being further removed by HF treatment, the alkanes decreased to 62.21% and the alkenes

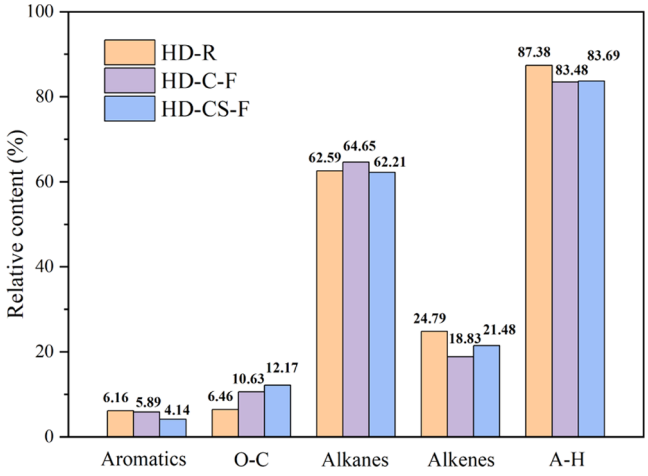

Figure 5. Relative content of major compounds in shale oils from GC−MS. (O-C: oxygenated compounds; A-H: aliphatic hydrocarbons).

increased to 21.48%. The existing research[35] pointed out that the formation of *n*-alkanes, *α*-olefins, and *n*-alcohols has homology, that is, the aliphatic group of kerogen breaks to form alkyl radicals, which can capture one hydrogen radical to form alkanes, or lose one hydrogen radical to form *α*-alkenes, or obtain one hydroxyl radical to form alcohols. As shown in Figure 6, during the co-current oxidizing pyrolysis of raw oil shale, alkaline and alkaline earth metal in carbonates will react with −COOH or −OH in organic matter to form exchangeable cations,[36] which will inhibit the efficient synthesis of hydrogen radicals and alkyl radicals, and simultaneously form more alkenes by releasing hydrogen radicals of alkyl radicals and reduce the alkanes. Similarly, according to the homology mechanism mentioned above, silicate is likely to promote the combination of hydrogen

https://doi.org/10.1021/acsomega.1c03098
ACS Omega 2021, 6, 23988−23997

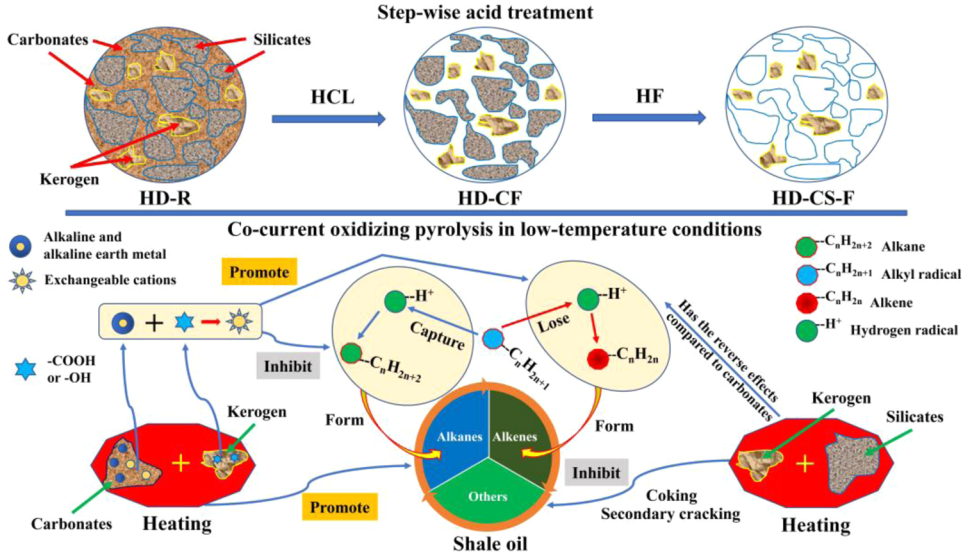

Figure 6. Description of the main phenomena occurring during the co-pyrolysis of kerogen and minerals in co-current oxidizing conditions.

radicals and alkyl radicals, which will increase the alkanes and decrease the alkenes in shale oil.[1]

Additionally, with the successive elimination of carbonates and silicates, the content of oxygen-containing compounds increased from 6.46 to 10.63 and 12.17%, respectively. These results are identical to the views that the decarboxylation of carboxylic acids to alkanes and the deoxidation of oxygenated compounds can be enhanced by the catalysis of clay minerals during the thermal decomposition of oil shale.[33,37] Furthermore, of particular concern is the content of aliphatic hydrocarbons for HD-C-F and HD-CS-F that decreased from 87.38 to 83.48 and 83.69%, respectively, and it appeared that the inhibition of minerals on the formation of aliphatic hydrocarbons was more significant than that of catalysis.

The saturate, asphaltene, resin, and aromatic (SARA) fractionation and characteristics of element composition of shale oils were also identified. Table 4 displays the results of the ultimate analyses of shale oils for raw oil shale and its demineralized products. It can be seen that the elimination of minerals resulted in different changes in the content of elements in shale oils, especially the organic carbon for HD-C-F has been significantly increased, indicating that carbonates could inhibit the conversion of organic carbon into shale oil. Further removal of the silicates reduced the proportion of organic carbon in shale oils compared with the hydrochloric acid-treated samples, suggesting that the silicates had promotional effects on the conversion process. At the same time, Table 4 also shows that the atomic ratio of H/C in shale oils had changed slightly.

Table 4. Ultimate Analyses of Shale Oils (wt %)[a]

						H/C	O/C
sample	C	N	H	S	O	atomic ratio, %	
HD-R	75.68	0.19	11.58	0.43	7.04	1.84	0.07
HD-C-F	80.93	0.58	11.90	0.53	4.55	1.77	0.04
HD-CS-F	75.09	0.05	11.66	0.44	5.86	1.86	0.06

[a]The data in the table are all measured values without normalization.

The four-component analysis can more intuitively and completely determine the content changes of heavy and light components in shale oil, avoiding the loss of the important information of heavy components during GC−MS analysis. The yields of SARA fractions (including saturates, aromatics, resin, and asphaltene) of shale oils are presented in Figure 7.

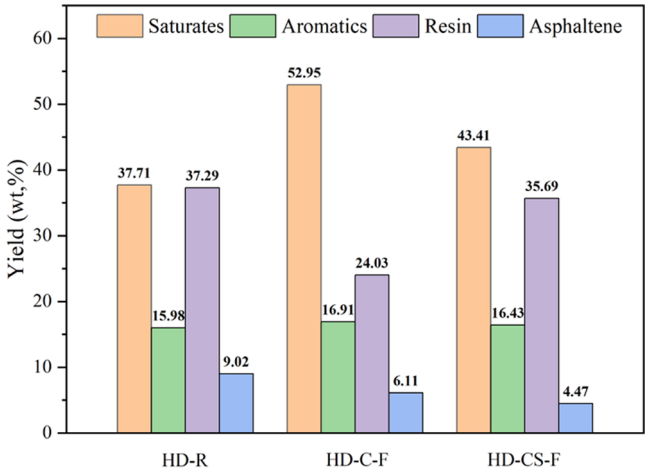

Figure 7. Yields of SARA fractions of shale oil samples.

Besides the saturates and aromatics, shale oil also contains considerable amounts of asphaltene and resin with high molecular weight. This is not consistent with the above results (Figures 4 and 5) because only the vital information about the light fraction compounds in shale oils can be detected via GC−MS as reported by Wang et al.,[38] who pointed out that shale oils derived from Huadian oil shale at a decomposition temperature of 520 °C only had a 47.2 wt % light fraction, which means that the components detected by GC−MS only account half for the total composition of shale oil.[33] The results of Figure 7 indicated that the removal of mineral substrates led to an increase in saturates compared with the raw oil shale, especially for HD-C-F, which means the presence of minerals would inhibit the formation of saturates in co-current oxidizing pyrolysis of oil shale. Meanwhile, the content of resin components in shale oils for HD-C-F and HD-C-S-F has been reduced to varying degrees. Moreover, the content of asphaltene in shale oils gradually decreased as the carbonates

https://doi.org/10.1021/acsomega.1c03098
ACS Omega 2021, 6, 23988−23997

and silicates were successively eliminated. To the best of our knowledge, asphaltene is the intermediate product of oil shale pyrolysis, which will be further converted into oil, gas, and residual carbon. Therefore, the reduction of asphaltene in shale oils indicated that the removal of minerals enhanced the conversion process of asphaltene, thereby reducing the proportion of macromolecular organic matter in shale oil and improving its quality.

2.3.2. Analysis of Noncondensable Gases. The change of gas components can be known via gas chromatography to detect the pyrolytic noncondensable gases obtained in the experiment. FID1 A, TCD2 B, and TCD3 C are front signal, rear signal, and auxiliary signal, respectively. As shown in Figure 8, the detected substances are mainly methane,

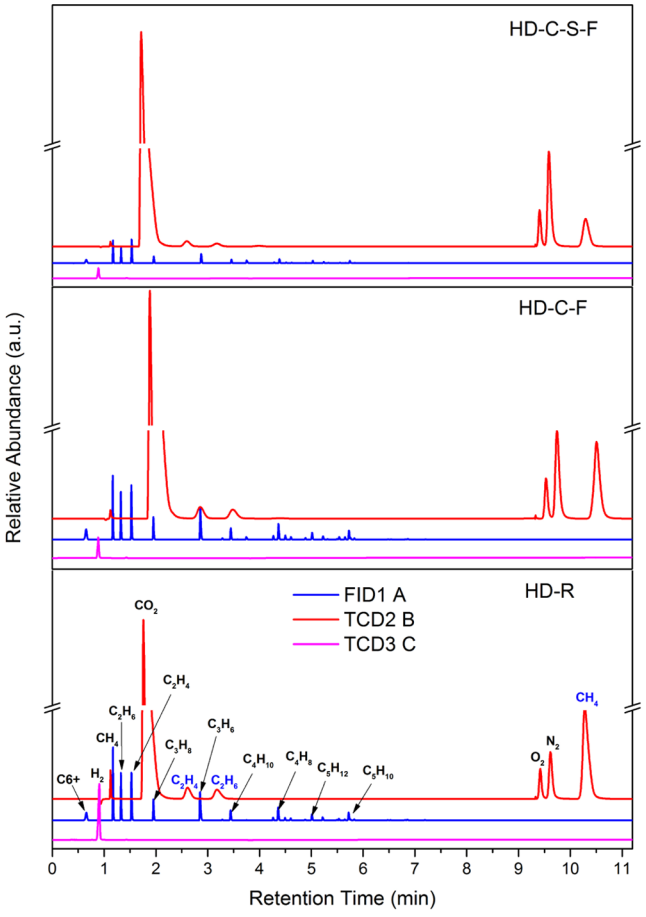

Figure 8. Gas chromatogram of noncondensable gases collected from the experiment.

hydrogen, carbon dioxide, and other organic gases (C_2H_4, C_2H_6, C_3H_6, C_3H_8, C_4H_8, C_4H_{10}, C_5H_{10}, C_5H_{12}). Unfortunately, no carbon monoxide has been identified in the spectra, and almost no sulfur dioxide or hydrogen sulfide was detected. The results also showed that the types, as well as the relative contents of organic gases, gradually decreased as most of the minerals (mainly carbonates and silicates) were eliminated.

It can be seen from Table 5 that the percentage of each compound in the pyrolytic noncondensable gases changed significantly after acid washing. The content of methane decreased from 8.1 to 4.29 and 2.96%, respectively, as the carbonate and silicate minerals were removed. Meanwhile, the removal of minerals also obviously reduced the content of

Table 5. Peak Area Percentages of Detected Components Present in Noncondensable Gases

	peak area percentage (%)		
major compounds	HD-R	HD-C-F	HD-CS-F
methane (CH_4)	8.12	4.29	2.96
hydrogen (H_2)	5.93	1.29	1.27
other organic gases (C_2–C_5)	12.59	8.58	7.18
carbon dioxide (CO_2)	73.36	85.84	88.59

hydrogen and other organic gases (C_2–C_5). Previous studies have shown that the coking reaction of oil and gas will lead to an increase in methane and hydrogen, and carbonates can reduce the content of methane and hydrogen by suppressing the coking reaction of oil and gas, while silicates have the opposite effect.[11,33] However, these reported conclusions are inconsistent with the results obtained in the present study. The possible reason for this is the removal of minerals that extends the retention time of pyrolytic products (more specifically, gaseous shale oil, CH_4, H_2, C_2–C_5) between the oil shale particles, making them unable to be discharged in time and thus be oxidized in the presence of oxygen, and ultimately leads to a reduction in their yield. Moreover, it can be further demonstrated that the content of carbon dioxide obviously increased from 73.36 to 85.84 and 88.59%, respectively, with the removal of a large number of minerals. In addition, the content of carbon dioxide in pyrolytic noncondensable gases for HD-R was much higher than that under retorting conditions,[21,33] which also proved that the fixed carbon (or semicoke) had been fully utilized via exothermic oxidation reaction during co-current oxidizing pyrolysis of oil shale.[10]

3. CONCLUSIONS

In the present work, the effects of associated minerals on the co-current oxidizing pyrolysis of oil shale in a low-temperature stage were explored based on the pyrolysis product yields and components. The obtained results present that the mineral matters have an essential effect on the distribution and composition of pyrolytic products. The removal of carbonates decreased the shale oil yield from 41.53% for HD-R to 22.38%, while it increased to 33.97% with the elimination of the silicate minerals (based on dry weight and mineral matter-free basis), indicating that carbonates promoted while silicates inhibited the formation of shale oil during the co-current oxidizing pyrolysis. A decrease of the alkanes and an increase of the alkenes of shale oil can be observed in the presence of carbonates via inhibiting the binding of the alkyl radical with the hydrogen radical by an exchangeable cation; however, the silicates have an inverse effect. Meanwhile, the silicates could enhance the conversion of organic carbon into shale oil and the conversion process has been strengthened after the carbonates were removed. From the SARA fractions of shale oils, it is found that the removal of minerals could promote the asphaltene conversion to shale oil, resulting in reducing the proportion of macromolecular organics in shale oil. The rapid increase of carbon dioxide and the decrease of organic gases in noncondensable gases could be attributed to more pyrolytic products being oxidized during co-current oxidizing pyrolysis with the elimination of most minerals. We hope that this study can provide a possible contribution to the development of oil shale conversion technology, especially when this high-efficiency method is used for in situ production of oil shale on a reservoir scale, a reasonable target reservoir pretreatment

https://doi.org/10.1021/acsomega.1c03098
ACS Omega 2021, 6, 23988−23997

can be formulated to achieve the purpose of efficient recovery of shale oil according to the distribution characteristics of pyrolysis products obtained under the effect of different associated minerals.

4. EXPERIMENTAL SECTION

4.1. Materials and Demineralization of Oil Shale. The raw oil shale samples, which were used in this study, were collected from the Huadian basin in Northeastern China. The oil shale sample was first dried at 60 °C and then crushed to pass through a sieve with 1 mm openings. The characterization of raw oil shale included proximate analyses, ultimate analyses, and the Fischer assay analyses, which are summarized in Table 6.

Table 6. Proximate, Ultimate, and Fischer Assay Analyses of Huadian Oil Shale

proximate analysis (wt %, ad)		ultimate analysis (wt %, ad)		Fischer assay analysis (wt %, ad)	
ash content	52.36	H	3.68	water	3.68
volatile matter	41.84	C	32.78	oil content	18.42
fixed carbon[a]	1.58	N	0.56	semicoke	68.53
moisture	4.22	S	1.75	gas	10.37

[a]Calculated by difference.

The acids used in this study include aqueous hydrochloric acid solution (HCl, 18.7 wt %) and a mixed solution of hydrochloric acid (HCl, 18.7 wt %) and hydrofluoric acid (HF, 41 wt %). First, 50 g of the raw oil shale (labeled HD-R) reacted with 600 mL of hydrochloric acid, stirred in a nitrogen atmosphere for 12 h at 70 °C to remove carbonate minerals. Then, the solid−liquid separation was performed, and the mixed samples were continuously washed with deionized water at 50−60 °C until the filtrate was neutral. Finally, the carbonate-free oil shale (labeled HD-C-F) can be gained after the filter residue is dried in an oven at 75 °C in vacuum conditions. To acquire the carbonate-silicate-free samples (labeled HD-CS-F), the HD-C-F samples were treated with a mixture of hydrochloric acid and hydrofluoric acid. Similarly, filtration and drying are required under the same experimental conditions.

4.2. Pyrolysis Experiment. The thermal decomposition of oil shale samples in different experimental conditions was carried out in a refitted aluminum retort furnace, which is schematically presented in Figure 9. The high-temperature reactor used in this study was made with a quartz tank (height: 120 mm; inner diameter: 60 mm), and a stainless-steel tube was placed at the bottom as the carrier gas inlet. In the pyrolysis experiments, the reactor was placed in an automatic temperature control device, which has a thermocouple placed inside the quartz tank and above the sample. Approximately 20 g of raw samples or the demineralization products was considered for each run. The device was heated from ambient temperature to 350 °C at a heating rate of 10 °C/min in a retorting atmosphere, and when it reached the target temperature, the pure oxygen with a flow rate of 80 mL/min was introduced to pass through the samples and remove the volatile products. The entire pyrolysis process lasted at 350 °C for 120 min to ensure the pyrolysis experiments be fully completed. It should be emphasized that after the sample is heated to the target temperature under inert conditions, the temperature of the heat source needs to be kept constant to ensure that no additional heat is injected into the reaction system, and then a fixed flow of pure oxygen at ambient temperature is introduced into the reactor to make it flow through the sample from the bottom up. The volatile pyrolytic products, including the oil vapor, water steam, and gases, are collected by the condensation device and air bags.

The solid residues and liquid products were entirely collected and accurately weighed to obtain the product yields. The separation of the oil and water was carried out in a toluene−water azeotrope. Then, the separated water was weighed and the oil yield can be obtained by difference. Finally, the yield of gas is gained via subtracting the weights of water, semicoke, and oil from the weight of the charge. The experiment of the same parameters should be repeated at least three times to ensure the accuracy and reproducibility of the pyrolysis experiments. The results indicated that the errors of quality were less than 1.5%. The formula for calculating the yield of pyrolysis products is as follows

$$Y_o = \frac{M_l - V_w \cdot \rho}{M_r} \times 100\% \quad (1)$$

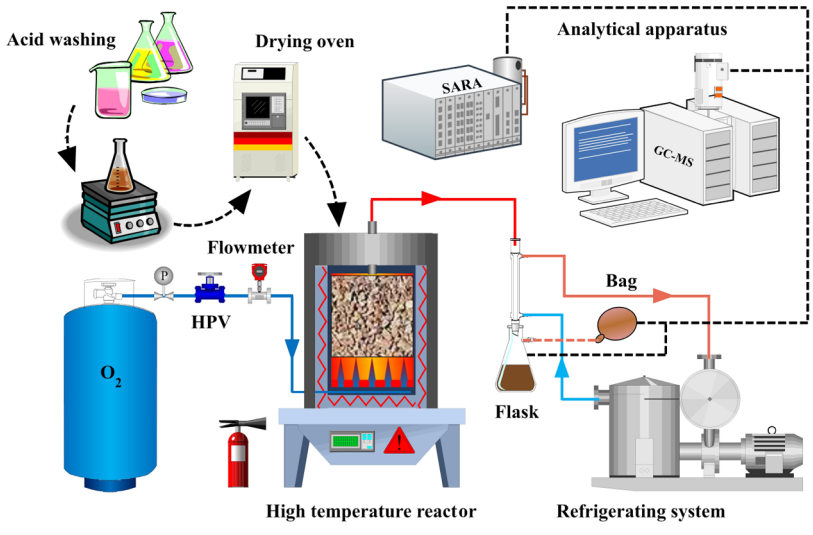

Figure 9. Schematic diagram of the experimental instruments used.

https://doi.org/10.1021/acsomega.1c03098
ACS Omega 2021, 6, 23988−23997

$$Y_w = \frac{V_w \cdot \rho}{M_r} \times 100\% \quad (2)$$

$$Y_s = \frac{M_s}{M_r} \times 100\% \quad (3)$$

$$Y_g = 1 - (Y_o + Y_w + Y_s) \quad (4)$$

where Y_o, Y_w, Y_s, and Y_g are the yield of shale oil, water, semicoke, and gas, respectively. M_r represents the quality of oil shale samples used for pyrolysis experiments, M_l and M_s represent the mass of liquid products and semicoke, respectively, V_w is the volume of water, and ρ is the water density of 298 K and 0.1 MPa.

4.3. Analytical Methods. The proximate, ultimate analyses of original and demineralized oil shales were carried out on an Arena 20 Automatic Industrial Analysis System (Thermo Fisher) and Elemental Analyzer (Vario EL, Germany), respectively. The identification of minerals presented in HD-R, HD-C-F, and HD-CS-F samples was performed using an X-ray diffraction instrument (XRD) with a Bruker D8 diffractometer using Cu Kα radiation in the 2θ range of 3−72°, with a step size of 0.04°. The detailed information of the pore structure of samples used was obtained from the N_2 adsorption/desorption experiment, which was carried out on the Surface Area and Porosity Analyzer (Micromeritics). Before the nitrogen adsorption measurement, the sample was crushed to 0.2−0.3 mm and degassed in a vacuum at 100 °C for 6 h. The Agilent's 7890-5975N gas chromatography−mass spectrometer (GC−MS) was performed to characterize the composition of shale oil. The information of the chemical class composition of dewatered shale oil was gained through the alumina adsorption chromatography column, and the shale oil was distinguished into saturate, asphaltene, resin, and aromatic (SARA) fractions to further understand the detailed characteristics. The noncondensable gases, including the hydrocarbon gases (CH_4, C_2H_6, C_2H_4, and so on) and the inorganic gases, for example, CO_2 and H_2, were measured with the Agilent's 7890A gas chromatograph (GC), which deployed a hydrogen flame ionization detector (FID).

AUTHOR INFORMATION

Corresponding Author

Wei Guo − *College of Construction Engineering, Jilin University, Changchun 130021, China; National-Local Joint Engineering Laboratory of In-situ Conversion, Drilling and Exploitation Technology for Oil Shale, Provincial and Ministerial Co-construction of Collaborative Innovation Center for Shale Oil & Gas Exploration and Development, and Key Laboratory of Ministry of Natural Resources for Drilling and Exploitation Technology in Complex Conditions, Jilin University, Changchun 130021, China;* orcid.org/0000-0001-8693-2156; Email: guowei6981@jlu.edu.cn

Authors

Qinchuan Yang − *College of Construction Engineering, Jilin University, Changchun 130021, China; National-Local Joint Engineering Laboratory of In-situ Conversion, Drilling and Exploitation Technology for Oil Shale, Provincial and Ministerial Co-construction of Collaborative Innovation Center for Shale Oil & Gas Exploration and Development, and Key Laboratory of Ministry of Natural Resources for Drilling and Exploitation Technology in Complex Conditions, Jilin University, Changchun 130021, China*

Mingyi Guo − *College of Construction Engineering, Jilin University, Changchun 130021, China; National-Local Joint Engineering Laboratory of In-situ Conversion, Drilling and Exploitation Technology for Oil Shale, Provincial and Ministerial Co-construction of Collaborative Innovation Center for Shale Oil & Gas Exploration and Development, and Key Laboratory of Ministry of Natural Resources for Drilling and Exploitation Technology in Complex Conditions, Jilin University, Changchun 130021, China;* orcid.org/0000-0002-3465-4585

Complete contact information is available at: https://pubs.acs.org/10.1021/acsomega.1c03098

Notes

The authors declare no competing financial interest.

ACKNOWLEDGMENTS

The authors would like to acknowledge the financial support from the National Key R&D Program of China (Grant No. 2019YFA0705502), the National Natural Science Foundation of China (NSFC, Grant No. 51604123), the Science and Technology Development Project of Jilin Province, China (Grant No. 20200201221JC), the Project of Jilin Province Development and Reform Commission of China, the Cooperative Project between Universities and Jilin Province, China (Grant No. SF2017-5-1), the Program for JLU Science and Technology Innovative Research Team (Grant No. 2017TD-13), the advisory research project of the Chinese Academy of Engineering (2019-XY-72), and the Fundamental Research Funds for the Central Universities.

REFERENCES

(1) Niu, M.; Wang, S.; Han, X.; Jiang, X. Yield and characteristics of shale oil from the retorting of oil shale and fine oil-shale ash mixtures. *Appl. Energy* **2013**, *111*, 234−239.

(2) Yang, Y.; Lu, X.; Wang, Q.; Mei, L.; Song, D.; Hong, Y. Experimental Study on Combustion of Low Calorific Oil Shale Semicoke in Fluidized Bed System. *Energy Fuels* **2016**, *30*, 9882−9890.

(3) Deng, S.; Wang, Z.; Gu, Q.; Meng, F.; Li, J.; Wang, H. Extracting hydrocarbons from Huadian oil shale by sub-critical water. *Fuel Process. Technol.* **2011**, *92*, 1062−1067.

(4) Allawzi, M.; Al-Otoom, A.; Allaboun, H.; Ajlouni, A.; Al Nseirat, F. CO2 supercritical fluid extraction of Jordanian oil shale utilizing different co-solvents. *Fuel Process. Technol.* **2011**, *92*, 2016−2023.

(5) Guo, H.; Lin, J.; Yang, Y.; Liu, Y. Effect of minerals on the self-heating retorting of oil shale: Self-heating effect and shale-oil production. *Fuel* **2014**, *118*, 186−193.

(6) Sun, Y.; Bai, F.; Liu, B.; Liu, Y.; Guo, M.; Guo, W.; Wang, Q.; Lü, X.; Yang, F.; Yang, Y. Characterization of the oil shale products derived via topochemical reaction method. *Fuel* **2014**, *115*, 338−346.

(7) Sun, Y. H.; Bai, F. T.; Lu, X. S.; Li, Q.; Liu, Y. M.; Guo, M. Y.; Guo, W.; Liu, B. C. A novel energy-efficient pyrolysis process: self-pyrolysis of oil shale triggered by topochemical heat in a horizontal fixed bed. *Sci. Rep.* **2015**, *5*, No. 8290.

(8) Guo, H.; Pei, Y.; Wang, K.; Cheng, Q.; Ding, Y.; Jin, Z.; Yang, Y.; Wu, Q.; Liu, Y. Identifying the reaction mechanism of oil-shale self-heating retorting by thermal analysis techniques. *Fuel* **2015**, *160*, 255−264.

(9) Guo, H.; Peng, S.; Lin, J.; Chang, J.; Lei, S.; Fan, T.; Liu, Y. Retorting Oil Shale by a Self-Heating Route. *Energy Fuels* **2013**, *27*, 2445−2451.

(10) Guo, W.; Yang, Q.; Sun, Y.; Xu, S.; Kang, S.; Lai, C.; Guo, M. Characteristics of low temperature co-current oxidizing pyrolysis of Huadian oil shale. *J. Anal. Appl. Pyrolysis* **2020**, *146*, No. 104759.
(11) Pan, L.; Dai, F.; Huang, J.; Liu, S.; Li, G. Study of the effect of mineral matters on the thermal decomposition of Jimsar oil shale using TG−MS. *Thermochim. Acta* **2016**, *627*−*629*, 31−38.
(12) Ballice, L. Effect of demineralization on yield and composition of the volatile products evolved from temperature-programmed pyrolysis of Beypazari (Turkey) Oil Shale. *Fuel Process. Technol.* **2005**, *86*, 673−690.
(13) Yan, J.; Jiang, X.; Han, X.; Liu, J. A TG−FTIR investigation to the catalytic effect of mineral matrix in oil shale on the pyrolysis and combustion of kerogen. *Fuel* **2013**, *104*, 307−317.
(14) Yürüm, Y.; Drory; Levy, M. Effect of acid dissolution on the mineral matrix and organic matter of Zefa EFE oil shale. *Fuel Process. Technol.* **1985**, *11*, 71−86.
(15) Borrego, A.; Prado, J.; Fuente, E. Pyrolytic behaviour of Spanish oil shales and their kerogens. *J. Anal. Appl. Pyrolysis* **2000**, *56*, 1−21.
(16) Sert, M.; Ballice, L.; Yuksel, M.; Saglam, M. Effect of mineral matter on product yield and composition at isothermal pyrolysis of turkish oil shales. *Oil Shale* **2009**, *26*, 463−474.
(17) Al-Harahsheh, M.; Al-Ayed, O.; Robinson, J.; Kingman, S.; Al-Harahsheh, A.; Tarawneh, K.; Saeid, A.; Barranco, R. Effect of demineralization and heating rate on the pyrolysis kinetics of Jordanian oil shales. *Fuel Process. Technol.* **2011**, *92*, 1805−1811.
(18) Aouad, A.; Bilali, L.; Benchanaa; Mokhlisse, A. Kinetic aspect of thermal decomposition of natural phosphate and its kerogen: influence of heating rate and mineral matter. *J. Therm. Anal. Calorim.* **2002**, *67*, 733−743.
(19) El Harfi, K.; Aboulkas, A. Study of the Kinetics and Mechanisms of Thermal Decomposition of Moroccan Tarfaya Oil Shale and Its Kerogen. *Oil Shale* **2008**, *25*, 426−443.
(20) Sağlam, M.; Yüksel, M.; Ballice, L.; Sert, M. The Effects of Acid Treatment on the Pyrolysis of GÖynÜk Oil Shale (Turkey) by Thermogravimetric Analysis. *Oil Shale* **2012**, *29*, 51−62.
(21) Wang, Q.; Zhang, H.; Chi, M.; Cui, D.; Xu, X. Effect of mineral matter on product evolution during pyrolysis of Huadian oil shale. *J. Fuel Chem. Technol.* **2016**, *44*, 328−334.
(22) Faisal, H. M. N.; Katti, K. S.; Katti, D. R. An insight into quartz mineral interactions with kerogen in Green River oil shale. *Int. J. Coal Geol.* **2021**, *238*, No. 103729.
(23) Alstadt, K. N.; Katti, D. R.; Katti, K. S. An in situ FTIR step-scan photoacoustic investigation of kerogen and minerals in oil shale. *Spectrochim. Acta, Part A* **2012**, *89*, 105−113.
(24) Alstadt, K. N.; Katti, K. S.; Katti, D. R. Nanoscale morphology of kerogen and in situ nanomechanical properties of Green River oil shale. *J. Nanomech. Micromech.* **2016**, *6*, No. 04015003.
(25) Chang, Z.; Chu, M.; Zhang, C.; Bai, S.; Lin, H.; Ma, L. Compositional and structural variations of bitumen and its interactions with mineral matters during Huadian oil shale pyrolysis. *Korean J. Chem. Eng.* **2017**, *34*, 3111−3118.
(26) Sun, B. Mineral Decomposition Characteristic Research of Oil Shale. Dissertation, Northeast Electric Power University: Jilin, 2013.
(27) Zhao, X.; Zhang, X.; Liu, Z.; Lu, Z.; Liu, Q. Organic Matter in Yilan Oil Shale: Characterization and Pyrolysis with or without Inorganic Minerals. *Energy Fuels* **2017**, *31*, 3784−3792.
(28) Lu, Z.; Zhao, X.; Liu, Z.; Liu, Q. Mutual Influences between Organic Matter and Minerals during Oil Shale Pyrolysis. *Energy Fuels* **2019**, *33*, 1850−1858.
(29) Hu, Y.; Zhao, Y.; Yang, D.; Kang, Z. Thermal Cracking and Corresponding Permeability of Fushun Oil Shale. *Oil Shale* **2011**, *28*, 273−283.
(30) Tiwari, P.; Deo, M.; Lin, C. L.; Miller, J. D. Characterization of oil shale pore structure before and after pyrolysis by using X-ray micro CT. *Fuel* **2013**, *107*, 547−554.
(31) Lu, L.; Kong, C.; Sahajwalla, V.; Harris, D. Char structural ordering during pyrolysis and combustion and its influence on char reactivity. *Fuel* **2002**, *81*, 1215−1225.
(32) Brunauer, S.; Deming, L.; Deming, We.; Teller, E. On a theory of the van der Waals adsorption of gases. *J. Am. Chem. Soc.* **1940**, *62*, 1723−1732.
(33) Chang, Z.; Chu, M.; Zhang, C.; Bai, S.; Lin, H.; Ma, L. Influence of inherent mineral matrix on the product yield and characterization from Huadian oil shale pyrolysis. *J. Anal. Appl. Pyrolysis* **2018**, *130*, 269−276.
(34) Kumar, R.; Bansal, V.; Badhe, R. M.; Madhira, I. S. S.; Sugumaran, V.; Ahmed, S.; Christopher, J.; Patel, M. B.; Basu, B. Characterization of Indian origin oil shale using advanced analytical techniques. *Fuel* **2013**, *113*, 610−616.
(35) Wang, Q.; Cui, D.; Chi, M.; Zhang, H.; Xu, X. Influence of final retorting temperature on composition and property of Huadian shale oil. *J. Chem. Eng.* **2015**, *66*, 2670−2677.
(36) Joseph, J. T.; Forrai, T. R. Effect of exchangeable cations on liquefaction of low rank coals. *Fuel* **1992**, *71*, 75−80.
(37) Tannenbaum, E.; Kaplan, I. R. Role of minerals in the thermal alteration of organic matter——I: generation of gases and condensates under dry condition. *Geochim. Cosmochim. Acta* **1985**, *49*, 2589−2604.
(38) Wang, S.; Jiang, X.; Han, X.; Tong, J. Effect of retorting temperature on product yield and characteristics of non-condensable gases and shale oil obtained by retorting Huadian oil shales. *Fuel Process. Technol.* **2014**, *121*, 9−15.

https://doi.org/10.1021/acsomega.1c03098
ACS Omega 2021, 6, 23988−23997